LAWRENCE
LIVERMORE
NATIONAL
LABORATORY

Porphyrin-based Photocatalytic Nanolithography

Jane P. Bearinger, Gary Stone, Lawrence C. Dugan, Bassem El Dasher, Cheryl Stockton, James W. Conway, Tobias Kuenzler, Jeffrey A. Hubbell

June 11, 2009

Disclaimer

This document was prepared as an account of work sponsored by an agency of the United States government. Neither the United States government nor Lawrence Livermore National Security, LLC, nor any of their employees makes any warranty, expressed or implied, or assumes any legal liability or responsibility for the accuracy, completeness, or usefulness of any information, apparatus, product, or process disclosed, or represents that its use would not infringe privately owned rights. Reference herein to any specific commercial product, process, or service by trade name, trademark, manufacturer, or otherwise does not necessarily constitute or imply its endorsement, recommendation, or favoring by the United States government or Lawrence Livermore National Security, LLC. The views and opinions of authors expressed herein do not necessarily state or reflect those of the United States government or Lawrence Livermore National Security, LLC, and shall not be used for advertising or product endorsement purposes.

Porphyrin-Based Photocatalytic Nanolithography: A New Fabrication Tool for Protein Arrays

Jane P. Bearinger†*, Gary Stone†, Lawrence C. Dugan†, Bassem El Dasher†, Cheryl Stockton†,

James W. Conway£, Tobias Kuenzlerζ, and Jeffrey A. Hubbell‡

 [*] Dr. Jane P. Bearinger Corresponding-Author
Lawrence Livermore National Laboratory
L-211, 7000 East Ave,
Livermore, CA, USA
E-mail: bearinger1@llnl.gov
(tel): 925-423-0321
(fax): 925-424-2778

†Mr. Gary Stone, Dr. Lawrence C. Dugan, Dr. Bassem El Dasher, Ms. Cheryl Stockton
Lawrence Livermore National Laboratory
7000 East Ave,
Livermore, CA, USA

£Dr. James W. Conway
Stanford Nanofabrication Facility
Stanford University
Palo Alto, CA, USA

ζDr. Tobias Kuenzler
Laboratory for Surface Science and Technology (LSST)
ETH Hönggerberg
HCI F536, CH-8093 Zurich (Switzerland)

‡Dr. Jeffery A. Hubbell
Institute of Bioengineering and Institute of Chemical Sciences and Engineering, Station 15 Ecole
Polytechnique Fédérale de Lausanne (EPFL)
CH-1015 Lausanne, Switzerland

Running title: PCNL for Protein Arrays

Abbreviations in order of appearance:

Photocatalytic lithography (PCL)

Photocatalytic nanolithography (PCNL)

atomic layer deposition (ALD)

titanium dioxide (TiO_2)

zirconium dioxide (ZrO_2)

light-emitting-diode (LED)

poly(propylene sulfide)-*bl*-poly(ethylene glycol) (PPS-PEG)

micro- or nano- electromechanical systems (MEMS or NEMS)

Magnesium Phthalocyanine (MgPC)

polyacrylamide P(AAm)

atomic force microscopy (AFM)

scanning electron microscope (SEM)

polyolefin plastomers (POP)

Reactive Ion Etching (RIE)

Ultra Pure Water (UPW)

Fluorescein isothiocyanate labeled IgG (FITC-IgG)

Computer-Aided Design (CAD)

Selective molecular assembly patterning (SMAP)

SUMMARY

Nanoarray fabrication is a multidisciplinary endeavor encompassing materials science, chemical engineering and biology. We form nanoarrays via a new technique, porphyrin-based photocatalytic nanolithography (PCNL). The nanoarrays, with controlled features as small as 200 nm, exhibit regularly ordered patterns and may be appropriate for (a) rapid and parallel proteomic screening of immobilized biomolecules, (b) protein-protein interactions and/or (c) biophysical and molecular biology studies involving spatially dictated ligand placement. We demonstrate protein immobilization utilizing nanoarrays fabricated via PCNL on silicon substrates, where the immobilized proteins are surrounded by a non-fouling polymer background.

INTRODUCTION

Biomolecular arrays facilitate molecular aggregate investigation and high throughput analysis of immobilized biomolecules. Current biomolecular arraying capabilities are limited by relatively large sample volumes (typical spot sizes are on the order of ~100-200 μm) and relatively long incubation times(1). In spite of their limitations, protein microarray applications include auto-antibody profiling, antibody response profiling, identification and detection of bacterial and protein analytes, as well as disease proteomics (oncoproteomics)(2-5). Typically, a specific analyte is bound and detected by fluorescence, resulting in an expression profile or protein atlas.

Nanoarrays are expected to expand the use of biomolecular arrays beyond drug discovery, medical diagnostics and genetic testing, to include point-of-care and in-the-field applications(6). We present a rapid and low-cost photocatalytic lithography method for generating biomolecular nanoarrays on a non-fouling background appropriate for analysis of immobilized biomolecules.

A number of publications have reviewed approaches to nanofabrication and bionanopatterning(7-9) of substrates including photolithography, contact printing(9, 10), imprint lithography(11-13), Dip-Pen lithography(14-17) and block co-polymer formation(18, 19). These approaches exhibit varying degrees of efficiency and success. Photocatalytic lithography (PCL) is a more recently described technique that is capable of generating arrays. Lee and Sung(20) patterned silane layers by activating TiO_2 (a photocatalytic semiconductor) via 2 min exposure to UV light. They produced approximately 600 nm parallel lines with 400 nm spaces, and they subsequently performed atomic layer deposition of ZrO_2 onto exposed silanol groups (alternating octadeclysiloxane regions did not have necessary precursor molecules). The subsequent decomposition of alkylsiloxane monolayers with TiO_2 was reported to be 20 times faster than under UV irradiation in air.

Previously, we have described patterning via porphyrin-based PCL(21). Patterning is achieved within 10 s and with extremely low energy sources (an LED flashlight is sufficient). As presented below, we have miniaturized features patterned with this new technique and are now able to pattern on the scale of 200 nm; this is roughly half the reported scale achieved with PCL using photocatalytic semiconductors. We refer to patterning on this scale as porphyrin-based photocatalytic nanolithography (PCNL). We describe the implementation of porphyrin-based PCNL to form large-scale nanoarrays appropriate for rapid, parallel, quantitative proteomic screening of immobilized biomolecules, and to form spatially dictated ligand arrays for functional proteomic studies.

EXPERIMENTAL PROCEDURES

Mask masters

Masters for the nanometer-scale structures were fabricated by electron-beam lithography (EBL) using a Raith150 system (Raith GmbH, Dortmund, Germany). After cleaning, the silicon masters were coated with a 264 nm thick ZEP-520 positive tone electron beam resist (ZEON Corp., Tokyo Japan) and soft baked for 120 s at 200 °C. Wafers were mounted on a leveled electrostatic chuck. The resist was exposed to an electron beam at an acceleration voltage of 20 kV using an electron dose of 70 µC cm^{-2}

for the grid pattern of Fig. 1, and using an electron dose of 250 μC cm^{-2} for the grid pattern shown in Fig. 3. After EBL exposure, the resist was developed in Xylenes for 40 s at 20 °C with gentle agitation, followed by soaking in 1:3 methyl isobutyl ketone/ isopropyl alcohol (MIBK/IPA) solution for 30 s, and then rinsed with pure 2-Propanol for 30 s to stop development.

After lithography, the wafers were soft baked at 90 °C for 2 min immediately before loading into an Applied Materials P-5000 MERIE system for Reactive Ion Etching. RIE was performed in a two-step process. The initial breakthrough step removed the intrinsic native silicon dioxide layer over the silicon substrate using CF4 for 5 s (100 mT, 250 W). This was followed by RIE of the silicon substrate using a 1:1 ratio of CL_2 to HBr for 1 min (100 mT, 250 W 40 Gauss magnetic field). Target depth was 250-300 nm. The ZEP-520 thin film was stripped using Piranha etchant (9:1 H_2SO_4: H_2O_2, 120 °C).

Photomask Fabrication

Affinity polyolefin plastomers (POP)(22) were used to construct nanoscale masks. These materials are co-polymers of ethylene and R-olefin (butane or octane) and undergo metallocene polymerization, which selectively polymerizes the ethylene and co-monomer sequences. POP pellets (Affinity EG8150 (stiffer) or 8200 (softer), Dow Chemical Company, Midland, MI) were melted into 40 x 20 x 5 mm blocks at 190 °C under a pressure of 4 bar using an appropriate metal template. Thin polyimide foils were placed between metal and melted polymer to avoid sticking. After cooling to room temperature, the solid polymer bars were removed from the template, rinsed with ethanol and dried under a stream of nitrogen. In the next step, the bars were placed over the e-beamed masters (10 x 10 mm) prior to placement between two silicon wafers. This "sandwich" was placed on a heatable plate (heated to 130 °C from both sides). A weight of 200 g was put on top of the sandwich for 5 min, followed by a weight of 700 g for 4 min. After cooling, the master was peeled off from the POP bar, which was then cut to its proper size with a razor blade. Prior to usage, the POP masks were cleaned with acetone for 5 min in an ultrasonic bath.

Substrate Preparation

Silicon (cut to approximately 1 cm^2, <100> Micralyne; Edmonton, Alberta, CA) substrates were placed in Fluoroware™ (Chaska, MN) baskets and sonicated first in UPW, then in 2-propanol and, finally in UPW (each step 10 min). The substrates were immersed in a Piranha etch bath comprised of concentrated H_2SO_4: 30% H_2O_2 (5:1 vol/vol%) for 20 min, followed by thorough rinsing in UPW. Substrates were individually blown dry under a filtered nitrogen stream and exposed to oxygen plasma (SPI, West Chester, PA) at 50 mA, 300 mTorr vacuum. As previously described, we grafted Allyltrichlorosilane (ATC, United Chemicals; Bristol, PA), prepared in anhydrous toluene (1.25% by volume) in a glove box purged with nitrogen, to the substrates(21, 23). Briefly, immobilization was performed in toluene for 1 min, followed by rinsing and a 5 min bake at 120 °C to accelerate bond formation.

Photocatalytic Nanolithography

We dissolved 1 mg/ml Magnesium Phthalocyanine (MgPC, Frontier Scientific, Logan, UT) in ethanol with sonication. A drop of solvated porphyrin was applied to the photomask and blown dry with nitrogen. Masks held by tweezers were carefully placed by hand on top of the ATC-coated Si chips.

Controlled patterning and removal of the ATC was achieved by local oxidation of the photocatalyst on the topographically patterned POP masks through 10 s illumination of the photocatalyst with an LED flashlight (Restoration Hardware; San Francisco, CA) exhibiting intensity peaks at 455 and 550 nm. Control experiments exposed ATC-coated substrates to photomasks without porphyrin in the presence of excitation energy (light). Selective patterning was not observed. Illumination with 660 nm red LED light (LUMEX; Glenview, IL; or Superbright LEDs; St. Louis, MO) also effectively achieved patterning.

Localized patterning and removal of the ATC occurred at locations in close contact to the excited porphyrin on the photomasks, i.e., occurred at elevated areas of the masks that were selectively created

from the Si masters. ATC areas positioned under recessed mask regions remained intact. After patterning, surfaces were sonicated in solvent for 1 min and blown dry with nitrogen.

Optical Microscopy

Surface patterning was monitored at each step of the patterning process by exposing the patterned substrates to water vapor(24) and acquiring images with a Nikon D100 camera mounted on a reflectance-based Nikon Labophot 2 microscope. A few images were acquired in quick succession after introduction of water vapor, in order to view differences in surface energy between patterned and background substrate regions.

Scanning Electron Microscopy (SEM)

An FEI Company Quanta 200 Environmental Scanning Electron Microscope (Hillsboro, Oregon) was used in high vacuum mode. Figures 1 and 2 include micrographs obtained using the secondary electron detector at 1kV and a spot size of approximately 100nm. No staining was necessary to image patterned polymer films; however, contrast was enhanced for the micrographs presented.

Atomic Force Microscopy (AFM)

Features on patterned silicon substrates were imaged using a Digital Instruments Dimension 3100 atomic force microscope (Digital Instruments/Veeco Metrology Group, Inc.; Santa Barbara, CA) with SiN (DNP-S) probes. Contact mode was used for friction and topography imaging. Image processing was peformed with WSxM 2.1 Scanning Probe Microscopy Software (www.nanotec.es).

Protein Adsorption

Fluorescently-labeled protein experiments were conducted by first immersing photocatalytically patterned substrates in a 25 µg/ml solution of recombinant Protein A (Pierce Biotechnologies; Rockford, IL) in PBS for approximately 1 h at room temperature. After thoroughly rinsing in PBS, the substrates were immersed in 50 µg/ml fluorescein isothiocyanate IgG (FITC-IgG, Santa Cruz Biotechnology, Inc.; Santa Cruz, CA) in PBS for 30 min. Photocatalytically patterned samples exposed to FITC-IgG were stored in polystyrene dishes sealed with parafilm and wrapped in aluminum foil to keep out light. Substrates subsequently were rinsed 3 times in PBS, then rinsed in distilled water and

dried before imaging. Detection of FITC-labeled IgG on surfaces exposed to fluorescently labeled proteins was achieved using a Roper Scientific Photometrics CoolSnap CCD camera (Tuscon, AZ) and Universal Imaging's Metamorph software (v 6.1). Images were acquired at 100x magnification, for 10,000 ms and binned 3x3. The detector had a well depth of 16 bits. Post acquisition, images were analyzed using Image J 1.40g and contrast was enhanced.

RESULTS

Creation of Nanoscale Arrays

Micron-scale PCL results have demonstrated the retained functionality, shape and spacing of patterns, proteins, prokaryotic and eukaryotic cells(21, 25). PCL employing poly(propylene sulfide)-*bl*-poly(ethylene glycol) (PPS-PEG) on gold substrates controls protein adsorption(26). Our present efforts show that PCL can dictate nanoscale protein patterning, thereby enabling biophysical and molecular biological studies involving spatially dictated ligand placement.

We used the organic semiconductor Magnesium Phthalocyanine, MgPC, to accomplish robust, reproducible and low cost substrate patterning down to line widths of 200 nm. We created transparent, 3-D polymeric photomasks by melting the polyolefin elastomer POP pellets into silicon masters created with an electron beam. MgPC solvated in ethanol was applied to the patterned side of the mask and blown dry with nitrogen. The masks were placed by hand onto silane-coated silicon substrates.

Light was shone through the transparent, patterned, MgPC-coated photomasks for approximately 10 s in order to locally oxidize substrate silane chemistry in close contact with the photomask, while leaving substrate silane chemistry disposed more distant from, and along recessed regions of, the patterned photomask intact. Our chosen silane chemistry was unsaturated so that we could graft polyacrylamide, P(AAm), to retained matrix silane in a subsequent step, in order to create a passivating background for protein nanoarray fabrication (Scheme 1). We used a suite of techniques to characterize masters and photomasks, pattern resolution, homogeneity, as well as the ability to pattern protein on the nanoscale.

Porphyrin-based PCNL utilizes materials with interesting physical properties and low material costs. The porphyrin MgPC is known in biotechnology as a photodynamic therapy molecule(27), and in nanotechnology as a gas sensing material(28); it is also used in solar cells(29-31). Advantageously, MgPC absorbs light in the visible spectrum and can be solvated, making it preferable to other semiconducting photocatalysts used for lithography, such as TiO_2(20, 32, 33).

Corroborative Feature Characterization

With reference to Fig. 1, we provide an assembly of atomic force microscopy (AFM), optical microscopy and low voltage scanning electron microscopy (SEM) images that reveal the integrity and reproducibility of 600 nm line width silicon lines, surrounded by a matrix of P(AAm) chemistry, using PCNL. An AFM of the POP mask is shown as a contact mode surface plot in Fig 1A. Fig. 1B shows the friction mode image of the photocatalytically patterned P(AAm) / silicon substrate. We found that friction mode provided more contrast than height mode in our contact mode force microscopy experiments.

An optical image acquired at 500x is depicted in Fig. 1C. This image was acquired after lightly hydrating the P(AAm)/Si patterned surface. As described by Lopez(24), condensation of a vapor to a liquid correlates with the molecular structure of the surface. Thus, light hydration is a fast, inexpensive and non-destructive technique that provides a valuable method for characterizing chemically patterned surfaces. In our case, the P(AAm) hydrogel absorbed water preferentially over the silicon lines and thus resulted in strong (time-dependent) optical contrast. Low voltage SEM was performed at 1 kV to convey the secondary electron contrast between the P(AAm) matrix and the semiconducting silicon lines ("L" boxes, Fig. 1D).

We also patterned features across a range of line widths and 160:1 2-dimensional aspect ratios (Figs. 2 and 3). The silicon slits surrounded by a P(AAm) matrix depicted in the low voltage SEM of Figure 2 ranged from 2.4 μm to 320 nm in line width. Squares surrounded by a similar matrix ranged from 1.7 μm to 340 nm in diameter. Since we performed microscopy at 1 kV, we did not need to coat our substrate. The P(AAm) matrix provides contrast against the silicon features, due to greater interaction

9

of carbon, nitrogen and oxygen atoms with the secondary electrons from the beam, as compared to the interaction of the silicon atoms with the secondary electrons from the beam.

Nanoscale Protein Arrays

Fig. 3 depicts AFM (A), CAD drawing (B) and fluorescent imaging (C) of both a field of 500 nm diameter spots and of various features, including a modified version of the Paul Klee work, "Lady Apart". The fluorescent protein spots demonstrate feasibility of a direct immunoassay architecture, immobilizing protein and then probing it with labeled antibody (commonly used in proteomic arrays). This construct has been used by Paweletz(34) and Madoz-Gurpide(35-37) for microarray-based cancer research, and has been documented by Pollard for clinical proteomics(38). A signal to noise ratio of 1.94 was calculated using the Histogram tool in Image J. Signal from n=12 spots from 16 pixel regions of interest was equal to 160.6±26.4. Background signal from n=12 spots from 16 pixel areas between regions of interest was equal to 82.8±22.7. Scale was from 0 to 255.

The modified "Lady Apart" figure demonstrates the ability to traverse the micron to submicron scale within the length and line width aspects of the figure. The figure is almost 30 μm tall, but the lines are only 200 nm wide. Broad, dynamic range of pattern size, and the spanning of such length scales, has been problematic in the past due to mask collapse(39). As noted, this work was done by placing masks onto substrates by hand, yet line widths of similar magnitude to those found in state-of-the-art integrated circuit (IC) chips were achieved.

Our results in Figure 3C demonstrate nanoscale protein arraying. Subsequent to PCNL, P(AAm) was grafted and crosslinked to the remaining silane, resulting in a patterned substrate of a non-fouling P(AAm) matrix and adhesive silicon/ SiO$_2$ features. Protein nanoarrays then were formed by first bathing the substrate in a single concentration of protein A and then a single concentration of FITC-IgG solution in buffer. As our present goal is demonstrating protein immobilization utilizing nanoarrays fabricated via PCNL, we intentionally conducted experiments with a single protein concentration and labeling molecule concentration, where fluorescence saturation makes it easy to see the strikingly small features.

While we did not attempt to multiplex our initial demonstration, we note that others have used teflon barriers to subdivide regions, allowing numerous interactions to be tested(40). Teflon barriers would be difficult to fabricate and assemble with sub-millimeter accuracy. While the PCNL technique does not easily allow for side by side (less than one micron spacing) placement of different proteins, we envision etching silicon or glass substrates before any chemistry has been performed to set up micron-scale physical boundaries. Within such boundaries, large nanoarrays or small microarrays then may be chemically fabricated in conjunction with PCNL to allow for reproducibility testing per protein, as well as protein multiplexing.

DISCUSSION

Formation of patterned substrates via PCNL provides a platform for protein *nano*arrays. Such nanoarrays could significantly advance the capabilities of, for example, quantitative proteomics, wherein agents capture target proteins from complex mixtures for protein detection and quantification. Quantitative proteomics typically utilizes protein-detecting *micro*arrays with spot sizes on the order of 100 μm(1, 41). Protein nanoarrays cover less than 0.1% of the surface area of today's microarray spots, while maintaining enough antibodies to provide a useful dynamic range. PCNL is well positioned to assist in the transition from microarray to nanoarray research, and may be used to obtain global proteome analysis or even small-scale, on-chip bio-reactors.

Lynch describes the useful limit of an individual antibody capture domain to be about 250 nm(42), which is on the scale of our protein arraying results described below. Lynch points out that, while even smaller, single molecule detection systems are seductive, they are subject to statistical difficulties and can actually lengthen experimental sampling time due to the necessity for repeated sampling in order to obtain diagnostic readout (below a threshold size, array spots lack an adequate number of active capture molecules and may, therefore, suffer from inaccurate quantitation and poor dynamic range(42).

Using fluorescence microscopy, we were able to detect the presence of protein down to 200 nm line widths (Fig. 3C). Signal from the FITC-IgG, bound to proteins on silicon, was easily detectable. Regular periodicity of 500 nm spots also was readily detectable. Although the emission region on the sample is not spatially resolved (emission is resolved as larger recorded line width with high contrast over background), the presence of 200 nm line width features is clearly ascertained in the AFM images of Fig. 3A. While such an approach of using a single concentration of protein may be relevant to protein-protein interactions or nanoscale ligand placement, we point out that concentration range and linear detection range analyses will be necessary to enable proteomic chip studies with the PCNL technique and proteins of interest. However, conventional microscopy cameras and detectors are not sufficient to complete such a study with spot sizes primarily between 200 to 500 nm and therefore these experiments are not straightforward to conduct. Fluorescence microscopy performed on 200-500 nm spot sizes can present a detection problem due to limited signal, if the recorded detector counts are not well above background. With spot sizes this small, cryogenically cooled detectors are required to image fluorescence in a quantifiable way. We plan a future series of studies that include a range of protein concentration and analysis of the linear detection range. For this set of experiments, we will appropriately design masks with spot sizes of approximately 600-800 nm so that the results are relevant to researchers with conventional biomedical imaging equipment, while still providing significantly higher density arrays than are available today.

One of the goals of proteomic research is to understand how proteins interact with each other and with other biomolecules to control processes at the cellular, tissue and whole organism level. Biomolecular arraying allows for molecular aggregate investigation (focal adhesions serve as one example of hierarchically-organized cooperation among proteins), as well as for high-throughput protein analysis. The effect of spatially positioning signaling cues at different length scales on cell response is a key question in the other branch of proteomics, known as functional proteomics. As with quantitative proteomics, PCNL is positioned to advance functional proteomic studies.

Synergistic interaction studies by Elbert(43), Irvine(44, 45), Koo(46), Maheshwari(47), Lussi(48), Irvine(44) and Arnold(49) provide initial insight into cell response to spatially positioned signals and suggest research avenues for directing cell adhesion through placement of nanoscale peptide and protein ligands. Cell adhesion and motility may be governed by growth factor receptors and integrin adhesion receptors interacting with the extracellular environment, followed by collaborative intracellular signaling(50). There is clearly a complex synergy between receptors and integrins, and modeling shows that spatial ligand presentation affects cell regulation behavior(51).

We believe that PCL/PCNL is well-suited for functional proteomic studies, as it can traverse the micron- to nano-scale patterning requirements incumbent in the design of substrates for such studies. We have previous experience creating cell arrays on the micron scale with PCL(21). Now that we have patterned on the nanoscale, we are positioned to control cell arrays on a much smaller scale by placing small molecule ligands or ligand clusters beneath patterned cells.

As seen in Scheme 2, we envision a 3 step process. First, porphyrin-based PCL exposes silicon substrate regions ranging from 20 μm (for single cell attachment) to 100 μm (for cell cluster attachment) on substrates homogenously coated with non-fouling chemistry, such as P(AAm), P(AAm)-co-EG(51), or PLL-g-PEG(52; 53). Second, silicon regions are coated with Fibronectin (Fn). Third, PCNL, performed with a secondary mask and a mask aligner, re-exposes a majority of the silicon, leaving nanoscale regions of fibronectin on cell adhesive silicon patches surrounded by non-fouling matrix. In such a way, PCL/PCNL may facilitate multidimensional parameter testing on the same substrate to examine cooperativity - not just among proteins, but among cell contacts, as well.

PCNL allows for patterning across multiple orders of magnitude, a range of substrates, and in an ambient environment with little energy input. However, we have found that, similar to contact printing techniques, lateral diffusion of materials not strongly bound to substrates can deleteriously influence pattern resolution. Smaller, tightly bound materials and covalently bound materials perform better than larger, more loosely bound materials, which may result in pattern blurring.

Also, similar to contact printing techniques, mask modulus influences pattern resolution (see supporting information). While the polyolefin elastomer POP proved sufficient for line widths down to a few hundred nanometers, future work should investigate new materials, such as polyimides or low viscosity monomers that may be UV cured, in order to fabricate higher modulus, transparent masks that should enable patterning of spot sizes 50 nm or smaller.

We note that all work done in our lab to date has utilized physical placement of mask materials on substrates by hand. We expect that the use of mask aligners to interface the mask and substrate would facilitate the higher resolution (estimated at less than 50 nm) that we believe is attainable with PCNL. Furthermore, all work done to date has relied on a thin layer of photosensitizer applied to masks via a volatile solvent film. We have performed preliminary experiments embedding photosensitizer within the masks and have found that (on the micron scale) they retain their function. We believe this may present a way of minimizing potential substrate contamination.

Biological applications for nanoarrays are increasing in both academia and industry, and biotechnology now plays a notable role in the chip fabrication market. Arriga(52) and Truskett(13) suggest that biotechnology is the future of nanoscale methods and applications. We have demonstrated that porphyrin-based PCNL is a rapid, low cost lithographic technique for nanoscale protein arraying on a non-fouling background, and we have reproducibly patterned protein on 200 nm diameter features. Porphyrin-based PCNL expands present nanoarray fabrication and proteomic study capabilities.

REFERENCES

1. Wingren, C. & Borrebaeck, C. A. K. (2007) Progress in miniaturization of protein arrays--a step closer to high-density nanoarrays, *Drug Discovery Today. 12*, 813-819.

2. Wingren, C. & Borrebaeck, C. A. K. (2006) Antibody microarrays: Current status and key technological advances, *OMICS A Journal of Integrative Biology. 10*, 411-427.

3. Haab, B. B. (2005) Antibody arrays in cancer research, *Molecular and Cellular Proteomics. 4*, 377-383.

4. Kingsmore, S. F. (2006) Multiplexed protein measurement: Technologies and applications of protein and antibody arrays, *Nature Reviews Drug Discovery. 5*, 310-320.

5. Borrebaeck, C. A. K. & Wingren, C. (2007) High-throughput proteomics using antibody microarrays: An update, *Expert Review of Molecular Diagnostics. 7*, 673-686.

6. Chen, H. & Li, J. (2007) Nanotechnology moving from microarrays toward nanoarrays, *Methods in Molecular Biology. 381*, 411-436.

7. Nie, Z. K., E. (2008) Patterning surfaces with functional polymers, *Nat. Matl. 7*, 277-290.

8. Mendes, P. M., Yeung, C. L. & Preece, J. A. (2007) Bio-nanopatterning of surfaces, *Nanoscale Research Letters. 2*, 373-384.

9. Gates, B. D., Xu, Q., Stewart, M., Ryan, D., Willson, C. G. & Whitesides, G. M. (2005) New approaches to nanofabrication: Molding, printing, and other techniques, *Chemical Reviews. 105*, 1171-1196.

10. Quist, A. P. P., E.; Oscarsson, S. (2005) Recent advances in microcontact printing, *Anal. Bioanal. Chem. 381*, 591-600.

11. Hoff, J. D., Cheng, L.-J., Meyhofer, E., Guo, L. J. & Hunt, A. J. (2004) Nanoscale Protein Patterning by Imprint Lithography, *Nano Lett. 4*, 853-857.

12. Blattler, T., Huwiler, C., Ochsner, M., Stadler, B., Solak, H., Voros, J. & Grandin, H. M. (2006) Nanopatterns with Biological Functions, *Journal of Nanoscience and Nanotechnology. 6*, 2237-2264.

13. Truskett, V. N. & Watts, M. P. C. (2006) Trends in imprint lithography for biological applications, *Trends in Biotechnology. 24*, 312-317.

14. Lee, K. B., Park, S. J., Mirkin, C. A., Smith, J. C. & Mrksich, M. (2002) Protein nanoarrays generated by dip-pen nanolithography, *Science. 295*, 1702-1705.

15. Lee, K. B., Lim, J. H. & Mirkin, C. A. (2003) Protein nanostructures formed via direct-write dip-pen nanolithography, *Journal of the American Chemical Society. 125*, 5588-5589.

16. Tinazli, A., Piehler, J., Beuttler, M., Guckenberger, R. & Tampe, R. (2007) Native protein nanolithography that can write, read and erase. *2*, 220-225.

17. Vega, R. A., Shen, C. K.-F., Maspoch, D., Robach, J. G., Lamb, R. A. & Mirkin, C. A. (2007) Monitoring single-cell infectivity from virus-particle nanoarrays fabricated by parallel dip-pen nanolithography, *Small. 3*, 1482-1485.

18. Kumar, N. & Hahm, J.-i. (2005) Nanoscale Protein Patterning Using Self-Assembled Diblock Copolymers, *Langmuir. 21*, 6652-6655.

19. Miller, A. C., Bennett, R. D., Hammond, P. T., Irvine, D. J. & Cohen, R. E. (2008) Functional nanocavity arrays via amphiphilic block copolymer thin films, *Macromolecules. 41*, 1739-1744.

20. Lee, J. P. & Sung, M. M. (2004) A new Patterning method using photocatalytic lithography and selective atomic layer deposition, *J. AM. CHEM. SOC. 126*, 28-29.

21. Bearinger, J. S., G; Christian, AT; Dugan, L; Hiddessen, AL; Wu, KJ; Wu, L; Hamilton, J; Stockton, C; Hubbell, JA. (2008) Porphyrin-Based Photocatalytic Lithography, *Langmuir. 24*, **5179 - 5184**.

22. Csucs, G., Kunzler, T., Feldman, K., Robin, F. & Spencer, N. D. (2003) Microcontact printing of macromolecules with submicrometer resolution by means of polyolefin stamps, *Langmuir. 19*, 6104-6109.

23. Bearinger, J. P., Castner, D. G., Golledge, S. L., Rezania, A., Hubchak, S. & Healy, K. E. (1997) P(AAm-co-EG) interpenetrating polymer networks grafted to oxide surfaces: Surface characterization, protein adsorption, and cell detachment studies, *Langmuir. 13*, 5175-5183.

24. Lopez, G. P., Biebuyck, H. A., Frisbie, C. D. & Whitesides, G. M. (1993) Imaging of Features on Surfaces by Condensation Figures, *Science. 260*, 647-649.

25. Bearinger, J. P., Dugan, L. C., Wu, L., Hill, H., Christian, A. T. & Hubbell, J. A. (2009) Chemical Tethering of Motile Bacteria to Silicon Surfaces, *Biotechniques. 46*, 209-216.

26. Bearinger, J. P., Stone, G., Hiddessen, A. L., Dugan, L. C., Wu, L., Hailey, P., Conway, J. W., Kunzler, T., Feller, L. M., Cerritelli, S. & Hubbell, J. A. (2009) Phototocatalytic Lithography of

Poly(Propylene Sulfide) Block Copolymers: Towards High Throughput Nanolithography for Biomolecular Arraying Applications, *Langmuir. 25*, 1238-1244.

27. Rosenthal, I. (1991) Phthalocyanines as photodynamic sensitizers, *Photochem. Photobiol. 53*, 859.

28. Miyata, T. & Minami, T. (2005) Chlorine gas sensors with high sensitivity using Mg-phthalocyanine thin films, *Applied Surface Science. 244*, 563-567.

29. Ingrosso, C., Petrella, A., Cosma, P., Curri, M. L., Striccoli, M. & Agostiano, A. (2006) Hybrid junctions of zinc(II) and magnesium(II) phthalocyanine with wide-band-gap semiconductor nano-oxides: Spectroscopic and photoelectrochemical characterization, *Journal of Physical Chemistry B. 110*, 24424-24432.

30. Riad, A. S., Elshabasy, M. & Abdellatif, R. M. (1993) Dc Electrical Measurements and Temperature-Dependence of the Schottky-Barrier Capacitance on Thin-Films of Beta-Mgpc Dispersed in Polycarbonate, *Thin Solid Films. 235*, 222-227.

31. Wagner, H. J. & Loutfy, R. O. (1982) Photoelectric Properties of Cds-Mgpc Heterojunction Solar-Cells, *Journal of Vacuum Science & Technology. 20*, 300-304.

32. Tatsuma, T., Kubo, W. & Fujishima, A. (2002) Patterning of solid surfaces by photocatalytic lithography based on the remote oxidation effect of TiO2, *Langmuir. 18*, 9632-9634.

33. Kubo, W., Tatsuma, T., Fujishima, A. & Kobayashi, H. (2004) Mechanisms and resolution of photocatalytic lithography, *J. Phys. Chem. B. 108*, 3005-3009.

34. Paweletz, C. P., Charboneau, L., Bichsel, V. E., Simone, N. L., Chen, T., Gillespie, J. W., Emmert-Buck, M. R., Roth, M. J., Petricoin, E. F. & Liotta, L. A. (2001) Reverse phase protein microarrays which capture disease progression show activation of pro-survival pathways at the cancer invasion front, *Oncogene. 20*, 1981-1989.

35. Madoz-Gurpide, J., Wang, H., Misek, D. E., Brichory, F. & Hanash, S. M. (2001) Protein based microarrays: A tool for probing the proteome of cancer cells and tissues, *Proteomics. 1*, 1279-1287.

36. Qiu, J., Madoz-Gurpide, J., Misek, D. E., Kuick, R., Brenner, D. E., Michailidis, G., Haab, B. B., Omenn, G. S. & Hanash, S. (2004) Development of natural protein microarrays for diagnosing cancer based on an antibody response to tumor antigens, *Journal of Proteome Research. 3*, 261-267.

37. Madoz-Gurpide, J., Kuick, R., Wang, H., Misek, D. E. & Hanash, S. M. (2008) Integral protein microarrays for the identification of lung cancer antigens in sera that induce a humoral immune response, *Molecular & Cellular Proteomics. 7*, 268-281.

38. Pollard, H. B., Srivastava, M., Eidelman, O., Jozwik, C., Rothwell, S. W., Mueller, G. R., Jacobowitz, D. M., Darling, T., Guggino, W. B., Wright, J., Zeitlin, P. L. & Paweletz, C. P. (2007) Protein microarray platforms for clinical proteomics, *Proteomics Clinical Applications. 1*, 934-952.

39. Michel, B., Bernard, A., Bietsch, A., Delamarche, E., Geissler, M., Juncker, D., Kind, H., Renault, J.-P., Rothuizen, H., Schmid, H., Schmidt-Winkel, P., Stutz, R. & Wolf, H. (2001) Printing meets lithography: Soft approaches to high-resolution printing, *IBM Journal of Research and Development. 45*, 697-719.

40. Schweitzer, B., Roberts, S., Grimwade, B., Shao, W. P., Wang, M. J., Fu, Q., Shu, Q. P., Laroche, I., Zhou, Z. M., Tchernev, V. T., Christiansen, J., Velleca, M. & Kingsmore, S. F. (2002) Multiplexed protein profiling on microarrays by rolling-circle amplification, *Nature Biotechnology. 20*, 359-365.

41. Kodadek, T. (2001) Protein microarrays: prospects and problems, *Chemistry & Biology. 8*, 105-115.

42. Lynch, M., Mosher, C., Huff, J., Nettikadan, S., Johnson, J. & Henderson, E. (2004) Functional protein nanoarrays for biomarker profiling, *Proteomics. 4*, 1695-1702.

43. Elbert, D. L. & Hubbell, J. A. (2001) Conjugate addition reactions combined with free-radical cross-linking for the design of materials for tissue engineering, *Biomacromolecules. 2*, 430-441.

44. Irvine, D. J., Mayes, A. M. & Griffith, L. G. (2001) Nanoscale clustering of RGD peptides at surfaces using comb polymers. 1. Synthesis and characterization of comb thin films, *Biomacromolecules. 2*, 85-94.

45. Irvine, D. J., Ruzette, A. V. G., Mayes, A. M. & Griffith, L. G. (2001) Nanoscale clustering of RGD peptides at surfaces using comb polymers. 2. Surface segregation of comb polymers in polylactide, *Biomacromolecules. 2*, 545-556.

46. Koo, L. Y., Irvine, D. J., Mayes, A. M., Lauffenburger, D. A. & Griffith, L. G. (2002) Co-regulation of cell adhesion by nanoscale RGD organization and mechanical stimulus, *Journal of Cell Science. 115*, 1423-1433.

47. Maheshwari, G., Brown, G., Lauffenburger, D. A., Wells, A. & Griffith, L. G. (2000) Cell adhesion and motility depend on nanoscale RGD clustering, *Journal of Cell Science. 113*, 1677-1686.

48. Lussi, J. W., Michel, R., Reviakine, I., Falconnet, D., Goessl, A., Csucs, G., Hubbell, J. A. & Textor, M. (2004) A novel generic platform for chemical patterning of surfaces, *Prog. Surf. Sci. 76*, 55-69.

49. Arnold, M., Cavalcanti-Adam, E. A., Glass, R., Blümmel, J., Eck, W., Kantlehner, M., Kessler, H. & Spatz, J. P. (2004) Activation of Integrin Function by Nanopatterned Adhesive Interfaces, *ChemPhysChem. 5*, 383-388.

50. Richardson, L. B. (2005) *EGF Receptor-mediated Fibroblast Signaling and Motility: Role of Nanoscale Spatial Ligand Organization*, MIT, Cambridge, MA.

51. Irvine, D. J., Hue, K. A., Mayes, A. M. & Griffith, L. G. (2002) Simulations of cell-surface integrin binding to nanoscale-clustered adhesion ligands., *Biophys J. 82*, 120-32.

52. Ariga, K., Nakanishi, T. & Michinobu, T. (2006) Immobilization of Biomaterials to Nano-Assembled Films (Self-Assembled Monolayers, Langmuir-Blodgett Films, and Layer-by-Layer Assemblies) and Their Related Functions, *Journal of Nanoscience and Nanotechnology. 6*, 2278-2301.

Dedication: This paper is dedicated to one of the fathers of Biomaterials, Professor Eugene Lautenschlager.

FIGURE CAPTIONS

Figure 1. Nanoscale Feature Characterization. A, AFM surface plot of POP mask repeat unit, line width = 600 nm; B, AFM friction mode image of photocatalytically patterned silicon substrate: "L" box is silicon, matrix is poly(acrylamide), scan width = 30 μm; C, optical image (500x optical zoom) of hydrated, photocatalytically patterned silicon substrate [poly(acrylamide) matrix is a water absorbing hydrogel, silicon "L" boxes do not absorb water and thus appear as bright lines]; D, low voltage secondary electron micrograph of poly(acrylamide)/ silicon [photocatalytically patterned "L" boxes are silicon; electrons preferentially interact with poly(acrylamide) hydrogel and convey higher intensity from matrix region].

Figure 2. Low voltage secondary electron micrograph of poly(acrylamide)/ silicon: photocatalytically patterned features are base silicon, electrons preferentially interact with poly(acrylamide) hydrogel and convey higher intensity from matrix region. Insets show contact mode AFM height images of POP mask slit and square features used for photocatalytic patterning experiments. MgPC was used as photocatalyst to oxidatively ablate silane on silicon. Poly(acrylamide) was then covalently grafted to remaining silane.

Figure 3. Nanoscale Protein Patterning. A, AFM surface plot height images of POP mask features used for patterning experiments B, CAD template for mask design (dot field comprised of 500 nm dia. Dots, 5 μm pitch; modified Paul Klee "Lady Apart" figure 32 μm long, 200 nm line width with 160:1 aspect

ratio). C, Fluorescence microscopy used to characterize poly(acrylamide)/ Si substrates exposed to FITC IgG. Magnification is 100x. Silane first photocatalytically patterned on Si (MgPC used as photocatalyst). Hydrogel then grafted to remaining silane. Substrate then exposed to fluorescent protein. Protein adsorbs to silicon (line widths 200 nm and above), but is repelled from hydrogel coated regions (matrix).

Scheme 1. Schematic of photocatalytic patterning process. Cross section (top), top down view (middle) and hydrated result after substrate exposure to water vapor (bottom): A, patterning process performed through PDMS photomask coated with photosensitizer from volatile solvent onto silane coated silicon substrate; B, patterned silane substrate upon selective silane removal from regions subjected to chemical decomposition by reactive oxygen species from excited photosensitizer; C, polymer grafting of thin acrylamide hydrogel layer onto remaining silane. Ls remain as Si/SiO$_2$ substrate.

Scheme 2. Experimental design for functional proteomic studies. Schematic of processing steps to generate nanoscale ligands on pre-dictated islands: A, cross sectional view; B), top down view C) exemplary substrates for single cell- (top) or cell cluster- (bottom) based islands (imaged HeLa cells patterned by PCL on silicon) with nanopatterned fibronectin (Fn) ligand placement (Ls) on substrate.

1) PCL exposes silicon substrate regions ranging from 20 μm (for single cell attachment) to 100 μm (for cell cluster attachment) on substrates homogenously coated with non-fouling chemistry.

2) Silicon regions are coated with Fn.

3) PCNL, performed with secondary mask and mask aligner, re-exposes majority of silicon, leaving nanoscale regions of Fn on cell adhesive silicon patches, surrounded by non-fouling matrix.
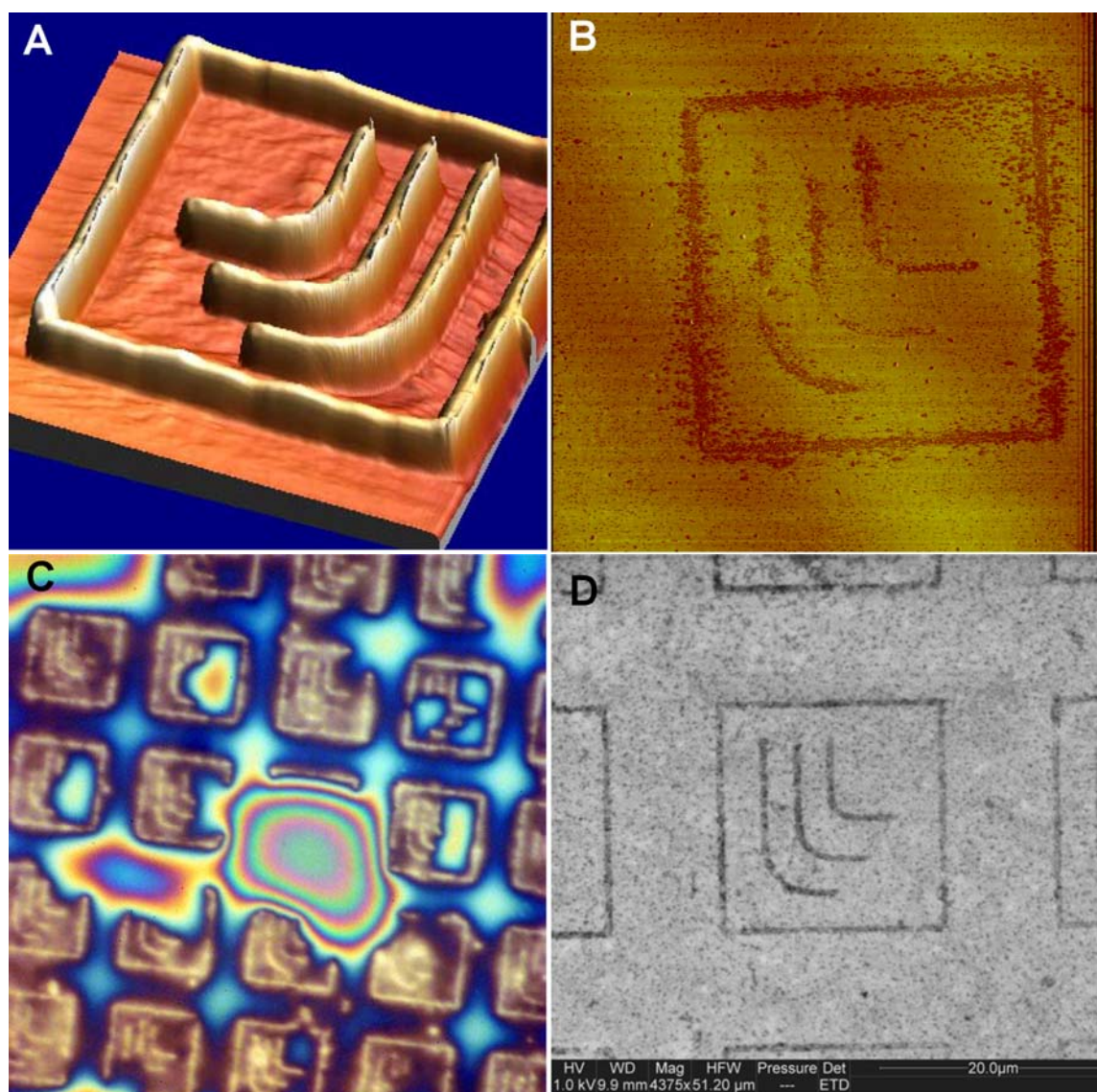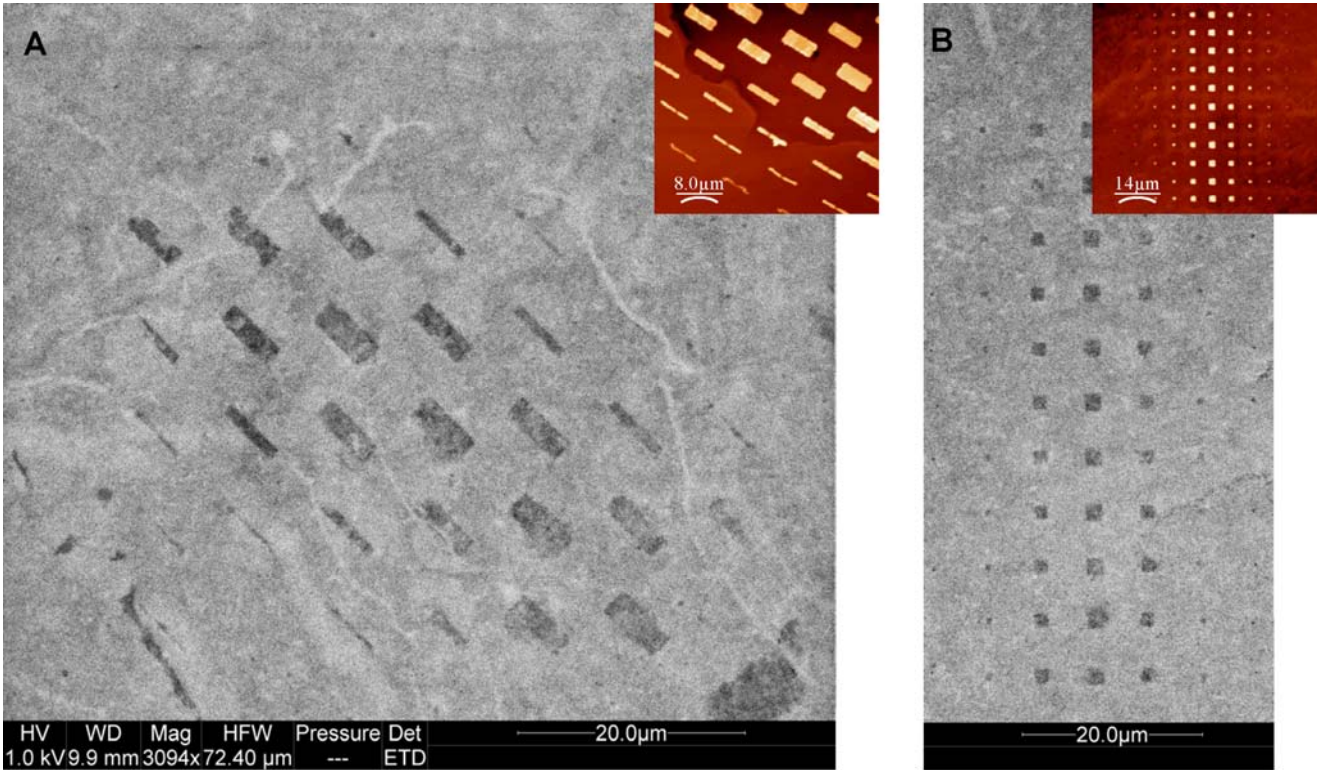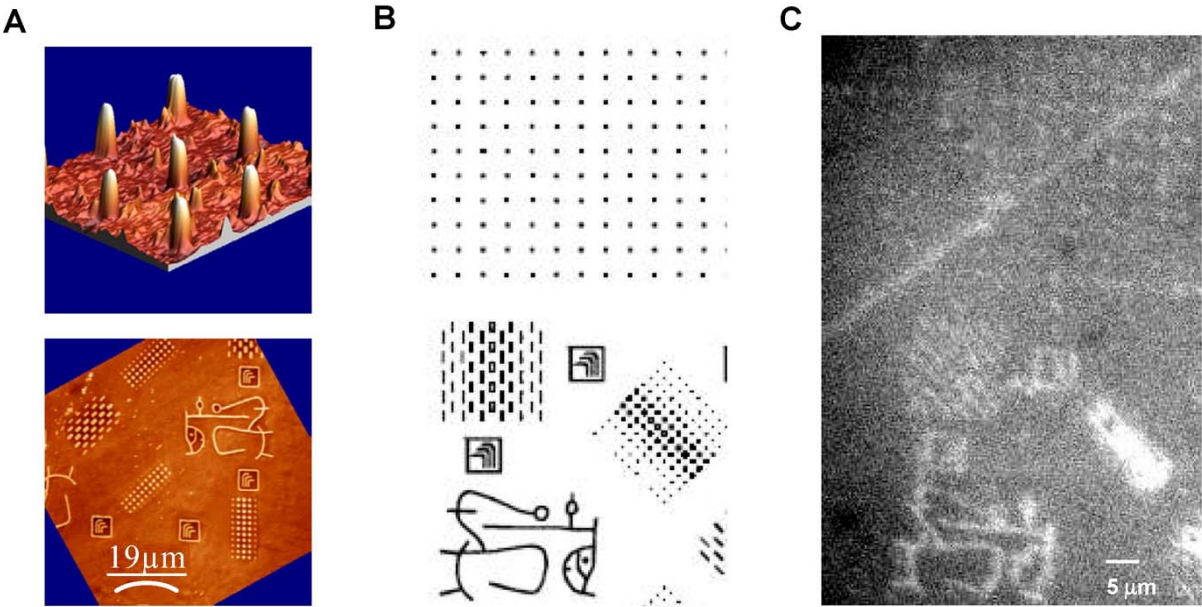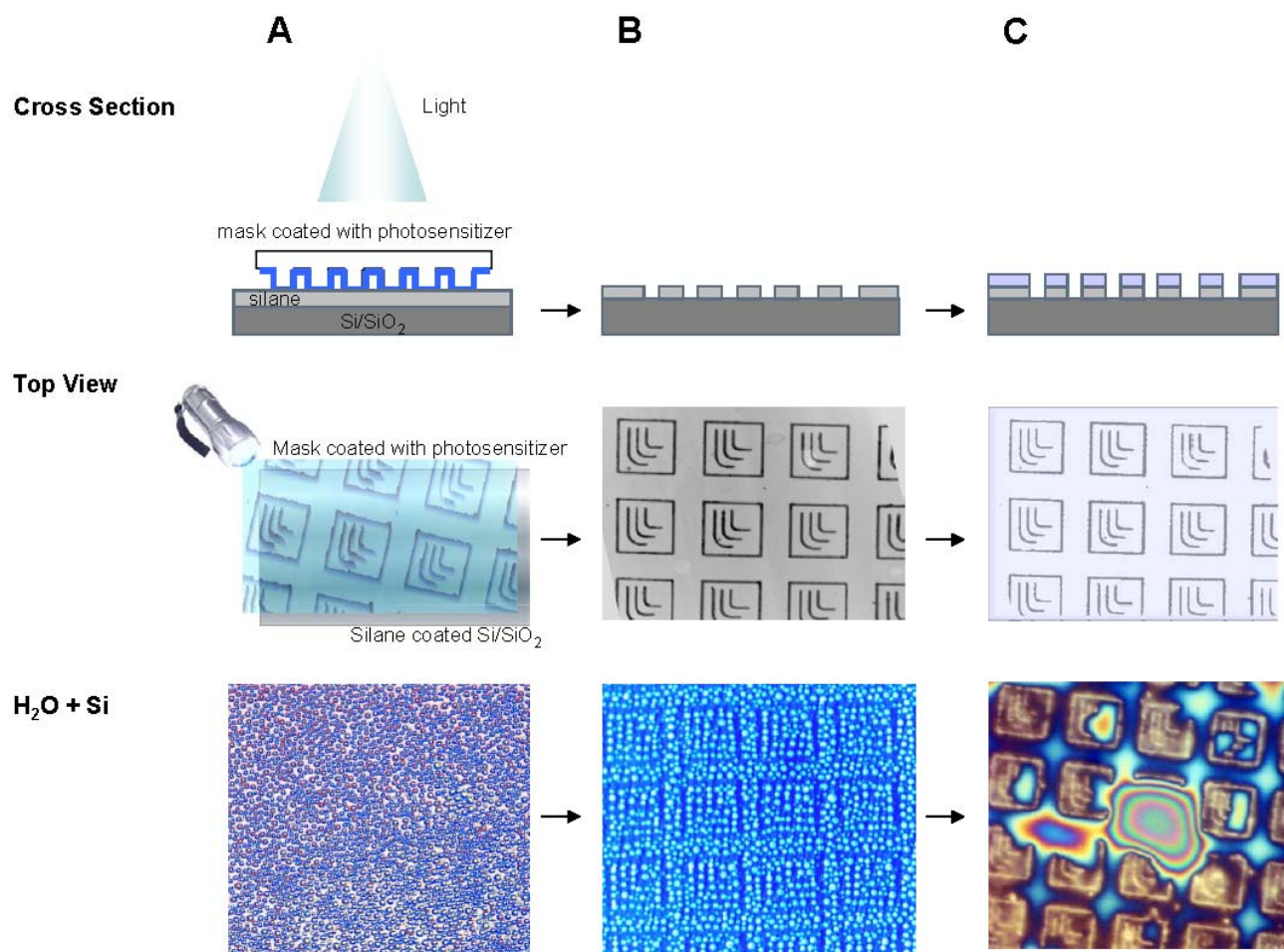
Figure 1

Figure 2

Figure 3

Scheme 1

	A	B	C
Cross Section			
Top View			
H₂O + Si			

Light

mask coated with photosensitizer

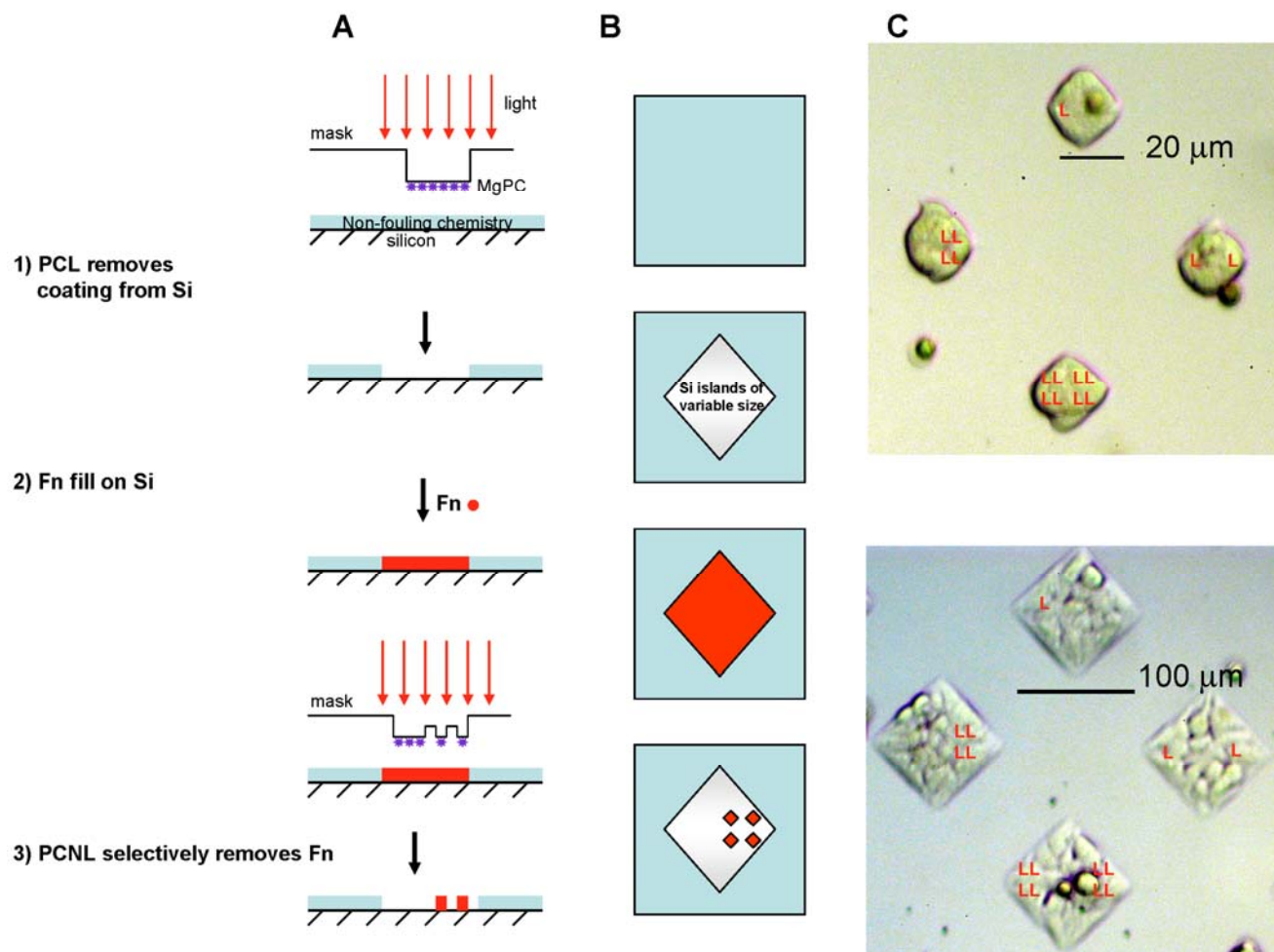silane

Si/SiO₂

Mask coated with photosensitizer
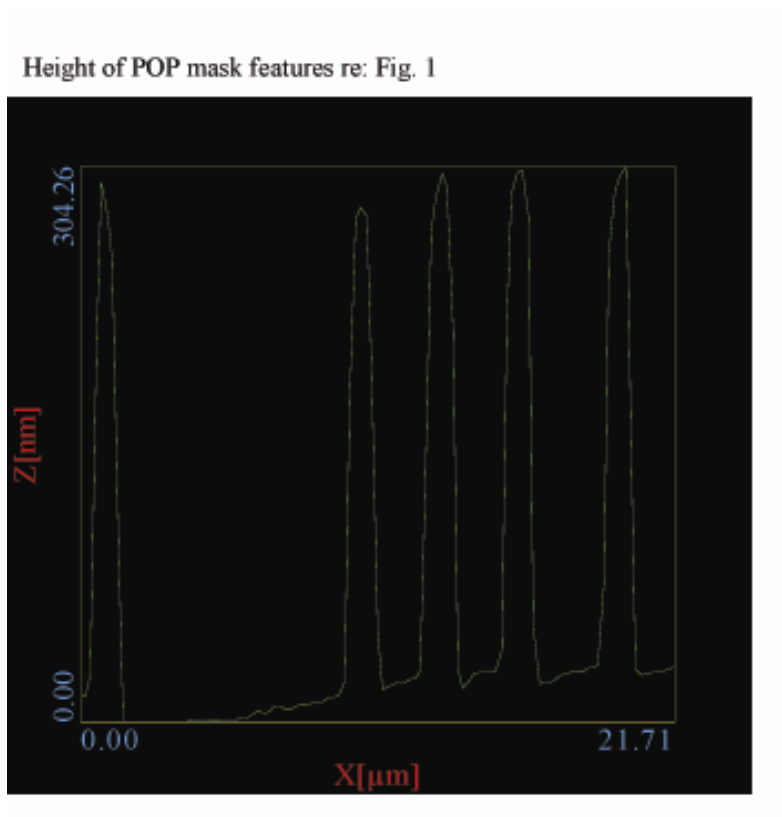
Silane coated Si/SiO₂

Scheme 2

Supporting Images:

Supporting images include more fluorescent protein images of nanoarray work to convey reproducibility, section analyses of contact mode AFM height images of masks, and deleterious effects (noted by low voltage SEM) of using a mask of lower moulus that leads to bowing on substrates.

1) Additional arrayed fluorescent protein images (note that some circular areas previously underwent photo bleaching due to image acquisition and long exposure times).

2) Section analyses of contact mode AFM height images of mask used in Fig. 1
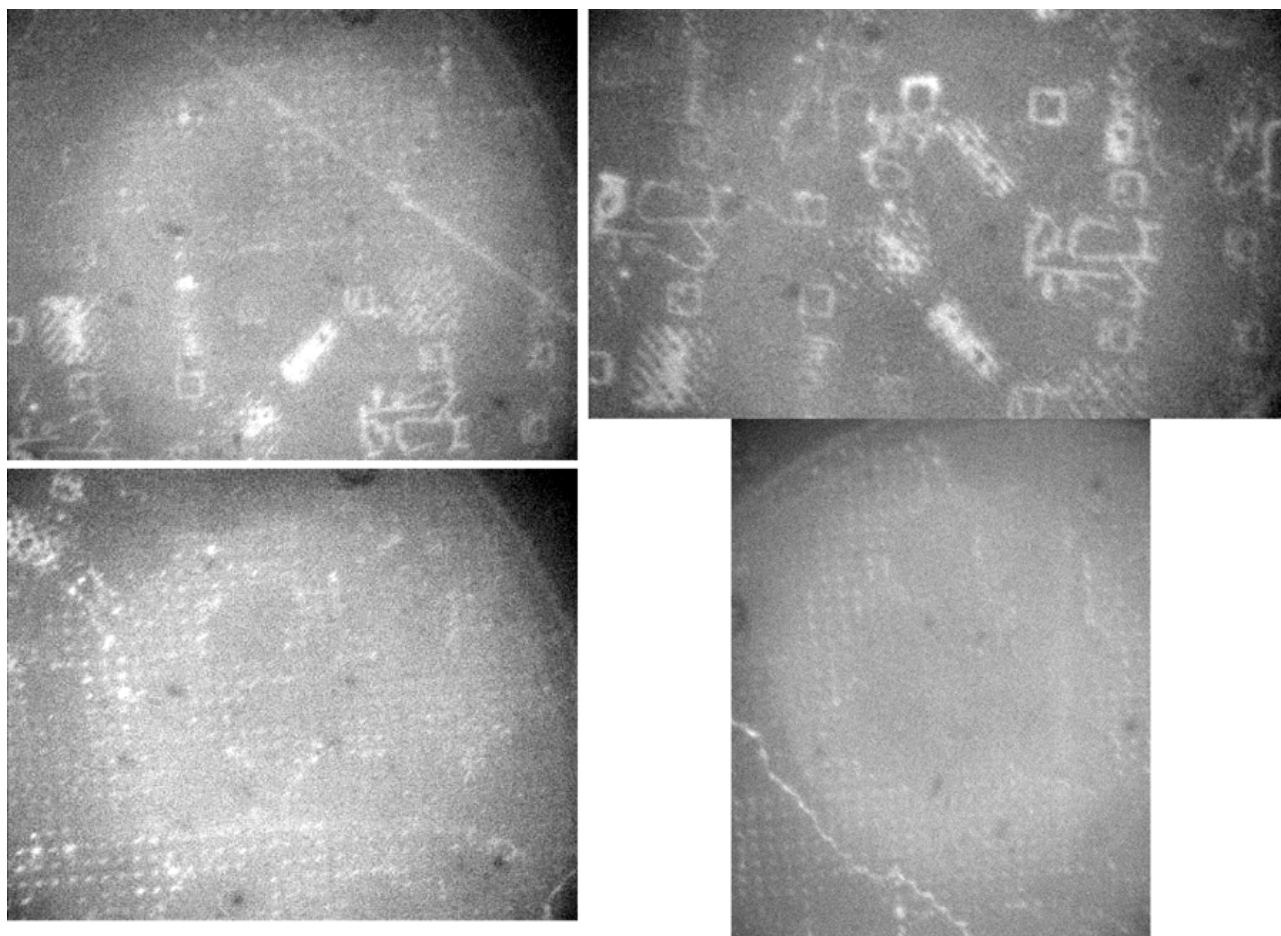
Height of POP mask features re: Fig. 1

3) Section analyses of contact mode AFM height images of mask used in Fig. 2

Height of POP mask features re: Fig. 2 (slits)
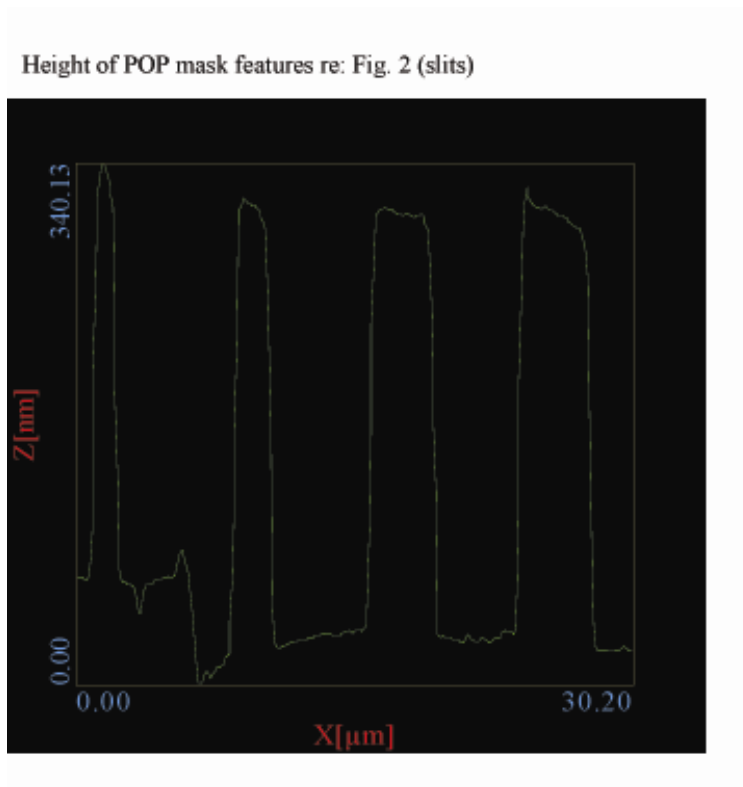
4) Deleterious effects (noted by low voltage SEM) of using a mask of lower modulus that leads to bowing on substrates

Affinity 8200 softer than 8150